Journal of Applied Mathematics and Physics, 2024, 12, 1819-1834
https://www.scirp.org/journal/jamp
ISSN Online: 2327-4379
ISSN Print: 2327-4352

Modeling the Physical Parameters of Solenoids for MEMS Applications

Mykhaylo Andriychuk[1,2], Bohdan Karkulovskyi[1], Yarko Kuleshnyk[1]

[1]Department of Computer Design System, Lviv Polytechnic National University, Lviv, Ukraine
[2]Department of Numerical Methods of Mathematical Physics, Pidstryhach Institute for Applied Problems of Mechanics and Mathematics, NASU, Lviv, Ukraine
Email: andr@iapmm.lviv.ua, bohdan.v.karkulovskyi@lpnu.ua, kuleschnyk@gmail.com

How to cite this paper: Andriychuk, M., Karkulovskyi, B. and Kuleshnyk, Y. (2024) Modeling the Physical Parameters of Solenoids for MEMS Applications. *Journal of Applied Mathematics and Physics*, **12**, 1819-1834.
https://doi.org/10.4236/jamp.2024.125113

Received: April 25, 2024
Accepted: May 26, 2024
Published: May 29, 2024

Abstract

The paper is devoted to study of the electrical parameters of the motion parts of the MEMS such as solenoids. The analytical background is given in order to describe the influence of the electrical field components on the forces, which are result of interaction of the electromagnetic (EM) field components with the parts of motion devices of MEMS. The given analytical formulas open the ability to calculate the self-inductance of the microsolenoids of the different kind, as well as the stored energy of such motion devices, that could be used for the modeling and optimization of parameters of running devices of MEMS such as actuators, sensors etc.

Keywords

EM Description, Motion Microdevice, Microsolenoid, Stored Energy, Computational Data

1. Introduction

The micro electromechanical systems (MEMS) are the series-fabricated integrated microdevices, which provide motion/motionless, radiating/fabricating energy, optical microdevices/microstructures, driving/sensing circuitry, and controlling/processing ICs that in the energy/motion relation provide, for example, the converting physical stimuli, events, and parameters to electrical, mechanical, and optical signals and vice versa.

MEMS are composed and built using microscale subsystems, devices, and structures. From the aforementioned sense, the MEMS, as the batch-fabricated integrated micro-system, can integrate particularly the following components: motion and motionless microdevices, radiating energy microdevices, energy

sources. The before mentioned explains, why the investigation of the MEMS parts related to electro dynamical and mechanical behavior is important. The strength of the MEMS devices rises during the last two decade owing the involvement of the electromagnetism principles with movement to the radiofrequency (RF) band of the power supplement. It is turned out that the stored energy of the EM field results in the moving process of the machine parts of MEMS components owing the appearing the mechanical forces in such parts, and vice versa, this moving could cause the appearing the EM fields in the moving mechanism. This is why the study of the EM field properties is important at the process of modeling and design of MEMS. One more aspect of MEMS is that in order to design effectively and with lower cost, there is necessity to use the mathematical modeling for the process.

Radiofrequency (RF) MEMS devices cannot be modeled precisely by measuring the data of small-signal S-parameters or large-signal commercial X-parameters, involving the designers of ICs to deal with the modeling methods. The S-parameters allow to evaluate only a low signal or linear behavior in the vicinity of an operating value, while the commercial X-parameters can cover the large signals or nonlinear properties, but have entanglement at delineating the long-term memory characteristics, when the extensions have been formulated [1]. This leads in the necessity to apply the adequate models, describing not the static nature of electrical processes only. The characteristics of independent memory are explained by the hysteresis curves, above result that the output of the device, which is path-dependent, must be in addition also input-dependent. One should note that the RF MEMS devices actuated electrostatically demonstrate a nonlinear behavior and associated hysteresis parameters.

To the recent time, the electrical behavior of the run parts of MEMS was considered from the static point of view, and taking into account of the dynamical nature of electromagnetic processes was limited.

In the electrostatically supported RF MEMS devices, the electrostatic forces are nonlinear and time varying (NLTV) having the pattern displacement and the drive voltage [2], [3]. They increase with voltage that leads to a square-law nonlinear characteristic, termed now as the electrostatic force strength growth. The RF MEMS devices actuated electrostatically and mainly all the capacitive transducers discover the electrostatic hysteresis behavior in the decapacitance-voltage plot [4]. The electrostatic hysteresis behavior that is result of the electrostatic force strength growth, provides the capacitance, which is a function of the imposed bias voltage, as well as of its previous condition, namely up-state or down-state. The strength of electrostatic force growth and respective hysteresis parameters characterize the pull-in and hold-down positions, and it designates a measure of linearity of the RF MEMS devices.

The second definitive discipline describing the MEMS run devices is micromechanics and forces acting on the MEMS elements. As a rule, such run is realized by the spring of the different kind. Notwithstanding that the spring force is usually linearized (the Hooke law of elasticity), it is a nonlinear with pattern dis-

placement [2], [3]. The nonlinear elastic behaviors are induced by spreading and other geometrical changes and the nonlinear material characteristics. The spreading produces the area and volume changes, and it depends on the dimensions of beam, suspension (spreading occurs usually for the beams having two and more clenches, for example the fixed-fixed beams), and mode of vibration (torsional, bulk or flexural). The spreading is one of main nonlinear elastic effects for the RF MEMS devices with flexural or deflecting mode at the appearance of the vibrating fixed-fixed beams, if they are produced of metal or polysilicon/single-crystal silicon.

The spreading presents a special attention while design the vibrating fixed-fixed pattern RF MEMS devices in a flexural mode. The respective positive force coefficient of cubic spring type leads to a spring-stiffening with displacement. And the spring-softening foresees a negative force coefficient, which is the result of a nonlinear modulus of Young only. The resonators, for which spring-softening and spring-stiffening is characteristic, are known as the "Duffing resonators". The spring-softening and the electrostatic force strength growth (using the Maclaurin series expansion) yields a positive force coefficient, but its constituents have opposite signs) that lowers the resonant frequency of Duffing resonator, while a spring-stiffening increases the above.

The nonlinear effects evoke a hysteresis amplitude-frequency curve, for which the mechanical resonant frequency is a multiple-valued function, which argument is the motive voltage amplitude. In order to hold out a non-linear oscillation, a Duffing resonator must have the limitation on amplitude at the input or a phase feedback circuit [5] in the case if it is used in an oscillator. The amplitude-frequency hysteresis characteristic is determinative when to calculate the minimal value of a phase noise or the frequency stability portion per million (PPM) of the oscillators related to the radiofrequency MEMS. The importance of taking into account of such non-linear effects caused by the interaction of the electrical and mechanical forces was noted in many publications [6]-[11] that evidences a hard necessity to design such models of run devices of MEMS, which take into account the interconnection of the electrical and mechanical forces very accurately. In this connection, the development of such models of MEMS, in which the run parts are designed accurately from the both electrical and mechanical point of view, is actual problem even in our time. In this paper we start with description of the electrical processes, which take place in the run parts of the different kind in MEMS. In particular, this approach is applicable for the study of the electrical properties of the solenoids of different kind. The sketch of solenoid with the circular cross-section is shown in **Figure 1**.

The solenoids are applied usually for interconnection of movable (plunger) and stationary (fixed) parts of MEMS and are produced of high-permeability ferromagnetic materials. The windings are wound with a helical rule as it is shown in **Figure 1**. The solenoids of such type convert electrical energy to mechanical energy or vice versa. The performance of solenoids are defined by the

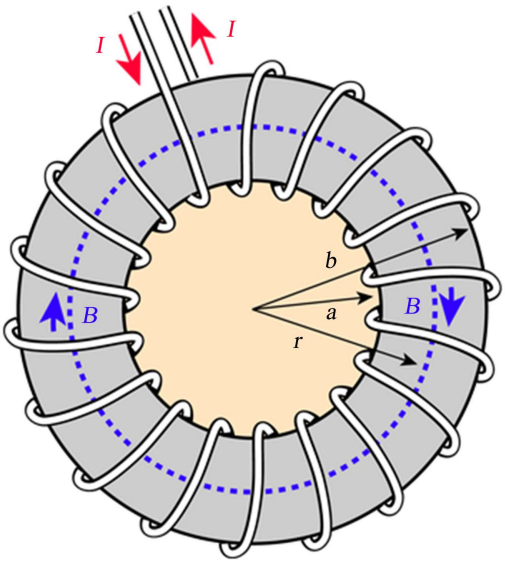

Figure 1. The sketch of microsolenoid with the circular cross-section.

electromagnetic system, materials, its geometry, magnetic permeability of material, resistance of winging, inductance of coil, friction of parts, and so on. The plunger is moving with respect to the stationary part. When the voltage is applied to the winding, the current flows in the winding, and the electromagnetic force appears resulting the moving of plunger. When the applied voltage diminishes, the plunger can return to its initial position because of the spring force. By this, the unacceptable effects like the residual magnetism and friction must be eliminated.

The different materials for design the central conductor (the nonmagnetic clutch) and plunger coating (the plating) must be chosen to get the minimum friction and to minimize wear. As a rule, the glass-filled nylon, brass for the guide and silver, copper, aluminum, tungsten, platinum plating, or other low friction materials are used for the plunger. For example, the friction coefficients of lubricated (solid film and oil) and unlubricated for different possible materials are used tungsten on tungsten 0.04 - 0.1 and 0.3; copper on copper 0.04 - 0.08 and 1.2 - 1.5; aluminum on aluminum 0.04 - 0.12 and 1; platinum on platinum 0.04 - 0.25 and 1.2; titanium on titanium 0.04 - 0.1 and 0.6, and so on. In this connection, the design, analysis, and optimization of the solenoids results in application of the basic physics, electromechanics, and production technologies. The above causes the compromise among a variety of mechanical, electrical, thermal, acoustical, and other physical properties.

2. The EM Characteristics of Solenoids

The electromagnetic field theory and mechanics are applied for study MEMS and NEMS, micro- and nanoscale devices and structures, ICs, and antennas. Electric force holds atoms and molecules together. Electromagnetics plays a central role in description of the power supplement of MEMS. Electric force is re-

sponsible for energy-transforming processes in the MEMS devices. The basics of EM theory are given in this Section provide with modeling the electrical parameters of the motion parts of MEMS. We follow the notations presented in [12]. We derive the formulas for the EM field characteristics that provide the ability to determine the energy and forces acting on the motion parts.

The influence of electromagnetic phenomena on the mechanical forces in MEMS was started within the electrostatic approximation introduced by Charles Coulomb. For charges q_1 and q_2, separated by a distance x in free space, the magnitude of the electric force F is

$$F = \frac{|q_1 q_2|}{4\pi\varepsilon_0 x^2}, \tag{1}$$

where ε_0 is the free space permittivity, $\varepsilon_0 = 8.85\times10^{-12}$ F/m or C^2/N·m, therefore $1/4\pi\varepsilon_0 = 9\times10^9$ N·m^2/C. The unit of force is Newton (N), and charge is measured in coulombs (C). Since force is vector, then the Formula (1) in order to accentuate this property, can be given as

$$\boldsymbol{F} = \frac{q_1 q_2}{4\pi\varepsilon_0 x^2}\boldsymbol{a}_x, \tag{2}$$

where $\boldsymbol{a}_x$ is unit vector directed along the line, with joins the points, where the charges q_1 and q_2 are applied.

The electric flux vector is $\boldsymbol{D}$ (F/m), and the vector of electric field intensity is $\boldsymbol{E}$ (V/m) or (N/C). According to Gauss's rule, the total electric flux Φ_e(C) across a closed surface is equal to the total force charge around and looks as

$$\Phi_e = \int_S \boldsymbol{D}\cdot \mathrm{d}\boldsymbol{S},\ \boldsymbol{D} = \varepsilon\boldsymbol{E}, \tag{3}$$

where $\mathrm{d}\boldsymbol{S}$ is surface area vector, $\mathrm{d}\boldsymbol{S} = \mathrm{d}s\boldsymbol{a}_N$, $\boldsymbol{a}_N$ is unit normal vector to surface S, ε is the permittivity of medium.

The magnetic flux Φ_m across the surface S is defined as

$$\Phi_m = \int_S \boldsymbol{B}\cdot \mathrm{d}\boldsymbol{S}, \tag{4}$$

where $\boldsymbol{B}$ is the density of magnetic flux.

$$\int_l \boldsymbol{B}\cdot \mathrm{d}\boldsymbol{l} = \mu_0 \int_S \boldsymbol{J}\cdot \mathrm{d}\boldsymbol{S}, \tag{5}$$

where μ_0 is the permeability of free space, and $\mu_0 = 4\pi\times10^{-7}$ H/m or T·m/A.

The vectors Φ_e and Φ_m have definitive role when the energy of electromagnetic field is defined and its relation to production of the mechanical forces is derived.

The law of Ampere in the case of the filamentary current couples the magnetic flux and the summarized enclosed or linked currents, termed as the net currents, i_n by

$$\oint_l \boldsymbol{B}\cdot \mathrm{d}\boldsymbol{l} = \mu_0 i_m. \tag{6}$$

The magnetic field, varying in time, creates the electromotive force (EMF) E

that produces some currents in the neighboring loop. The law of Faraday connects the EMF, which characterizes the induced voltage be presence of the magnetic field conductor motion, with the measure of changing the magnetic flux, which penetrates the loop. Using the approximate analysis of the conversion of electromechanical energy, we use the law of Lenz to determine the EMF vector and the induced current. Especially, the EMF is desirable in the direction, which provides some current with flux, when it is supplemented with the original flux, could decrease the EMF amplitude.

By the law of Faraday, the closed-loop circuit induced EMF is defined using the scale of the magnetic flux Φ change. This yield

$$\mathrm{E} = \oint_l E(t)\,\mathrm{d}t = -\frac{\mathrm{d}}{\mathrm{d}t}\int_S B(t)\,\mathrm{d}S = -N\frac{\mathrm{d}\Phi}{\mathrm{d}t} = -\frac{\mathrm{d}\Psi}{\mathrm{d}t}, \tag{7}$$

N is the turn's number, and Ψ corresponds to the linkages of flux. Formula (7) introduces the induction law of Faraday, therefore the induced EMF or induced voltage has form

$$\mathrm{E} = -\frac{\mathrm{d}\Psi}{\mathrm{d}t} = -N\frac{\mathrm{d}\Phi}{\mathrm{d}t} \tag{8}$$

in our consideration.

The vector of current and the linkages of flux are opposite directed. Therefore, the electromotive force, namely the energy per unit quantity of charge, is an amplitude of the difference of potential in a loop supporting the currents. Therefore

$$V = -ir + \mathrm{E} = -ir - \frac{\mathrm{d}\Psi}{\mathrm{d}t}. \tag{9}$$

The EMF is measured in volts.

The voltage law of Kirchhoff sets that across the closed path of a electric circuit, the total EMF is calculated as the vector sum of voltage come down through the resistance. The equivalent state is that the vector sum of the voltages nearby a closed contour in a circuit is equal to zero. The current law of Kirchhoff sets that the vector sum of currents in any circuit node is equal to zero.

The arising magnetomotive force (MMF) is the curved integral of the intensity $H(t)$ of magnetic field, which is time-varying. Namely,

$$\mathrm{MMF} = \int_l \boldsymbol{H}(t)\,\mathrm{d}\boldsymbol{l}. \tag{10}$$

One can conclude that the induced MMF is a sum of an induced current and the change scale of the flux, which transfuses across the surface of the boundary. To illustrate this clearly, we use the theorem of Stoke to reduce the law of Ampere in the integral form (that is the Maxwell second equation), which has form

$$\int_l \boldsymbol{H}(t)\cdot\mathrm{d}\boldsymbol{l} = \int_S \boldsymbol{J}(t)\cdot\mathrm{d}\boldsymbol{S} + \int_S \frac{\mathrm{d}\boldsymbol{D}(t)}{\mathrm{d}t}\cdot\mathrm{d}\boldsymbol{S}, \tag{11}$$

where $\boldsymbol{J}(t)$ denotes the current density vector, which is the time-varying. The magnetomotive force is measured in the amperes or the ampere-turns.

The dual nature of both the EMF and MMF characteristics is detecting if to

use two relations presented below, in the terms of field intensity of the vectors of electric and magnetic field

$$\mathrm{E}=\oint_l \boldsymbol{E}(t)\cdot \mathrm{d}\boldsymbol{l},\ \mathrm{MMF}=\oint_l \boldsymbol{H}(t)\cdot \mathrm{d}\boldsymbol{l}. \tag{12}$$

The value of inductance, namely the ratio of total linkage of flux to a current, which they join, is expressed as $L=N\Phi/i$); and the reluctance, namely the ratio of MMF to a whole flux, is given as $\mathrm{P}=\mathrm{MMF}/\Phi$. Both they are used to calculate the values of the EMF and MMF. Applying the formula $L=\Psi/i$ for the self-inductance, we get

$$\mathrm{E}=-\frac{\mathrm{d}\Psi}{\mathrm{d}t}=-\frac{\mathrm{d}(Li)}{\mathrm{d}t}=-L\frac{\mathrm{d}i}{\mathrm{d}t}-i\frac{\mathrm{d}L}{\mathrm{d}t}. \tag{13}$$

In the case when $L=\mathrm{const}$, we have $\mathrm{E}=-L\mathrm{d}i/\mathrm{d}t$. Namely, the self-inductance is equivalent to the self-induced EMF by unity of the current change.

The EMF and MMF can be related to the mechanical forces when the value of the energy stored by the electrostatic and magnetic fields. Formulas (25) - (28) in section below explain such interconnection.

3. EM Model of Toroidal Solenoid

The self-inductance of the motion devices is a definitive characteristic, which provide the information about the impact on its run performances. Let us get a representation for the toroidal solenoid self-inductance with a rectangular cross section with the size parameters 2*a*, *b*, and radius *r*.

The magnetic flux across the patch is

$$\mathrm{E}=\oint_l \boldsymbol{E}(t)\cdot \mathrm{d}\boldsymbol{l},\ \mathrm{MMF}=\oint_l \boldsymbol{H}(t)\cdot \mathrm{d}\boldsymbol{l}. \tag{14}$$

Thus

$$L=\frac{N\Phi}{i}=\frac{\mu N^2 b}{2\pi}\ln\left(\frac{r+a}{r-a}\right). \tag{15}$$

It is well-known that the electromagnetic torque $\boldsymbol{T}$ (in [N-m]) in the loop of current is:

$$\boldsymbol{T}=\boldsymbol{M}\times\boldsymbol{B}, \tag{16}$$

and $\boldsymbol{M}$ means the magnetic moment.

Let us give the torque-energy formulas related to micro- and nanoscale actuators. We find the relation for the energy of EM field. We know that an energy reserved by the capacitor is equal to $1/2CV^2$, and the energy reserved by the inductor is equal to $1/2Li^2$. The capacitor energy is reserved in the electric field between planes, and the inductor energy is reserved in the magnetic field across the coils.

We derive the formulas for both the energies reserved in both the electrostatic and magnetic fields through the field values. The total potential energy reserved in an electrostatic field is expressed by the difference of potential *V*. Basing on the above, we get

$$W_e = \frac{1}{2}\int_v \rho_v V \mathrm{d}v \left[\mathrm{J}\right], \tag{17}$$

and ρ_v is the density of volume charge [C/m^3], $\rho_v = \nabla \cdot \boldsymbol{D}$, and ∇ is the curl (rotor) operator.

Therefore, the potential energy W_e can be calculated by the work's quantity, which is needed to support the charge in the electrostatic field. For this end, the work's value is determined as the effect of the charge and potential.

In the area with a continuous distribution of charge ($\rho_v = \text{const}$), the charges are substituted by the value of $\rho_v \mathrm{d}v$, which results in the equation:

$$W_e = \frac{1}{2}\int_v \rho_v V \mathrm{d}v. \tag{18}$$

We get such formula for the energy reserved in the electrostatic field in the Gauss form:

$$W_e = \frac{1}{2}\int_v \boldsymbol{D}\cdot\boldsymbol{E}\mathrm{d}v, \tag{19}$$

using the relations $\rho_v = \nabla \cdot \boldsymbol{D}$ and $\boldsymbol{E} = -\nabla V$. By this, the electrostatic volume density of energy is given by $1/2\,\boldsymbol{D}\cdot\boldsymbol{E}$ (in [J/m^3]).

We get in the case of a linear isotropic medium

$$W_e = \frac{1}{2}\int_v \varepsilon \left|\boldsymbol{E}\right|^2 \mathrm{d}v = \frac{1}{2}\int_v \frac{1}{\varepsilon}\left|\boldsymbol{D}\right|^2 \mathrm{d}v. \tag{20}$$

The vector $\boldsymbol{E}(x,y,z)$ of electric field is determined by the function of scalar electrostatic potential $V(x, y, z)$:

$$\boldsymbol{E}(x,y,z) = -\nabla V(x,y,z). \tag{21}$$

For the cases of cylindrical and spherical coordinates, one gets

$$\boldsymbol{E}(r,\varphi,z) = -\nabla V(r,\varphi,z), \tag{22}$$

$$\boldsymbol{E}(r,\theta,\varphi) = -\nabla V(r,\theta,\varphi). \tag{23}$$

Using (18), the potential energy, which is reserved by the electric field in the vicinity of two surfaces is expressed as

$$W_e = \frac{1}{2}QV = \frac{1}{2}CV^2 \tag{24}$$

(this formula is used usually for a capacitor).

For the case of lossless conservative system, basing on the criterion of a virtual work, one can conclude that the total change of the electrostatic energy $\mathrm{d}W_e$ is the same that the total change of the mechanical energy $\mathrm{d}W_{mech}$. These yields

$$\mathrm{d}W_e = \mathrm{d}W_{mech}. \tag{25}$$

We get for a translational motion:

$$\mathrm{d}W_{mech} = \boldsymbol{F}_e \cdot \mathrm{d}\boldsymbol{l}, \tag{26}$$

and $\mathrm{d}\boldsymbol{l}$ is a differential displacement.

Using (25) and (26), we get $\mathrm{d}W_e = \nabla W_e \cdot \mathrm{d}\boldsymbol{l}$. Consequently, the force is de-

termined as the gradient of reserved electrostatic energy:

$$\boldsymbol{F}_e = \nabla W_e . \tag{27}$$

For the case of Cartesian coordinate system, we get

$$F_{ex} = \frac{\partial W_e}{\partial x}, \quad F_{ey} = \frac{\partial W_e}{\partial y}, \text{ and } \quad F_{ez} = \frac{\partial W_e}{\partial z}. \tag{28}$$

In such a way, the mechanical forces are determined by the stored EM field energy, which depends on the electric and magnetic vectors. The Formulas (20), (27), and (28) accentuate this interconnection. In the next Section, we get the explicit formulas for the components H_φ, E_θ, and E_r of EM field, which allow to calculate the stored energy of the electric and magnetic fields in the near and far zones. Having such components, relation (20), and formulas (28), we can easily to calculate the impact of the stored EM energy on the mechanical characteristics of the moving parts of MEMS.

4. Deriving the Formula for the Field Energy

The calculation of the energy of the EM field produced by the constituent parts of the MEMS motion machines has a important value for the modeling of its functioning. The calculation of energy when the self-capacitance is known foresees knowing the currents i (remembering formula $W = 1/2\,Li^2$ for capacitors). The above foresees the conducting the experimental data to define value of i. In many cases, the analytical formulas like (20) are used to calculate this characteristic. In the case of toroidal solenoid, the components of EM field can be calculated as [13]

$$\begin{aligned} H_\varphi = {} & \frac{\Lambda}{2r^3}\left[\left((kr)^2 - 1\right)\sin\Omega + kr\cos\Omega\right] J_1\left(kd\sin\theta\right) \\ & + \frac{\Lambda kd}{4r^3}\sin\Omega\sin\theta J_0\left(kd\sin\theta\right), \end{aligned} \tag{29}$$

$$\begin{aligned} E_\theta = {} & \frac{\Lambda k}{2r^2}\cos\Omega\left(J_1\left(kd\sin\theta\right) - kd\sin\theta J_2 V\left(kd\sin\theta\right)\right) \\ & - \frac{\Lambda k}{4r^3}\sin\Omega\left[d\sin\theta\left(J_0\left(kd\sin\theta\right) - 3J_2\left(kd\sin\theta\right) - 2kr^2 J_1\left(kd\sin\theta\right)\right)\right], \end{aligned} \tag{30}$$

$$\begin{aligned} E_r = {} & -\frac{\Lambda kd\cos\theta}{2r^3}\left(\sin\Omega - kr\cos\Omega\right) J_0\left(kd\sin\theta\right) \\ & + \frac{\Lambda kd^2\sin\theta\cos\theta}{2r^4}\left(3\cos\Omega + 2kr\sin\Omega\right) J_1\left(kd\sin\theta\right), \end{aligned} \tag{31}$$

where $\Lambda = \pi R^2 g$, $g = 2NI/c$, $\Omega = kr - \omega t$. The parameter R correspond to the torus, N is number of coils, I is the current in the separate coil, c is speed of light, ω is the angular frequency ($\omega = 2\pi f$), r is the distance to points of observation, t is time.

In a far zone

$$E_\theta = H_\varphi = \frac{1}{2r}\Lambda k^2 \sin\Omega J_1\left(kd\sin\theta\right), \tag{32}$$

$$E_r = \frac{1}{2r^2}\Lambda k^2 d\cos\theta\cos\Omega J_0\left(kd\sin\theta\right), \tag{33}$$

The Poynting vector's radial component is

$$P_r = \frac{1}{4\pi c}E_\theta H_\varphi = \frac{1}{4\pi c}\left(\frac{\Lambda k^2\sin\Omega}{2r}\right)^2\left(J_1\left(kd\sin\theta\right)\right)^2, \tag{34}$$

and it is calculated easily in such consideration. The integral energy flow is calculated as

$$WF = \frac{1}{4c}\left(\frac{\Lambda k^2}{2}\right)^2\int_0^\pi\left(J_1\left(kd\sin\theta\right)\right)^2\sin\theta\mathrm{d}\theta. \tag{35}$$

The last formula is related to one period. Having the Formulas (29) - (35), we can calculate the power characteristics of the MEMS running parts and use the obtained data for their optimization.

5. Numerical Modeling

The numerical data presented in this Section demonstrate the possibility to easy calculation of the characteristics of EM field and use them for optimization of the respective motion machines.

5.1. Calculation of the Self-Inductance of Rectangular Solenoid

The numerical data discussed in this Subsection present how the self-inductance L depends on the geometrical parameters of solenoid. The simple calculation formula is helpful when the optimization problem with respect to the above parameters is solved. The numerical results concern to study of dependence of the self-inductance L (Formula (15)) of the toroidal solenoid with the rectangular cross section $2a\times b$ on the parameters of problem. In **Figure 2**, the dependence of the self-inductance L on the number N of turns is shown for the different radius r at the fixed $a = 400$ nm and $b = 200$ nm. One can see that the value of L decreases if the radius r grows.

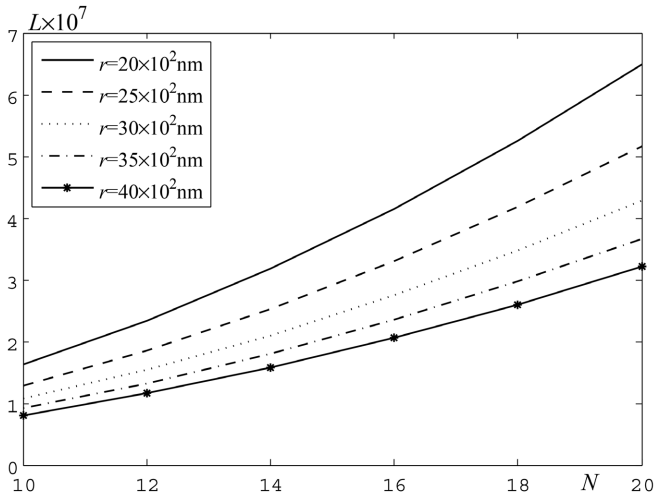

Figure 2. The self-inductance L versus rhe number N of turns.

Simultaneously, the value of L grows with increase of N. The characteristic of L approaches to the linear distribution when r increases. One can see that the change of L does not depend on r. The increase of L is the same for the different r, and it is close to four time. The dependence of L on the size a of the rectangle is shown in Figure 2 at the different r, $b = 200$ nm as in Figure 3.

The data presented in Figure 2 and Figure 3 testify that the values of L changes in a narrow range. It is evidently from the physical point of view that to increase L it is necessary to diminish a free space inside of solenoid, namely to increase size a remaining the radius r fixed. In Figure 4, the results demonstrated the change of L at the decreasing free space interior of solenoid are presented. The numerical results show that the self- inductance grows simultaneously with increase of number N of turns. One can note that the change of L is similar at the larger and smaller N, so, it increases to four times comparing the initial and final values.

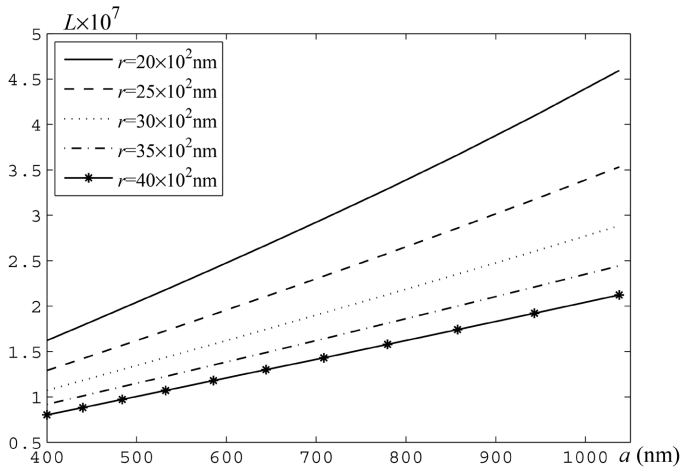

Figure 3. The self-inductance L versus rhe size a.

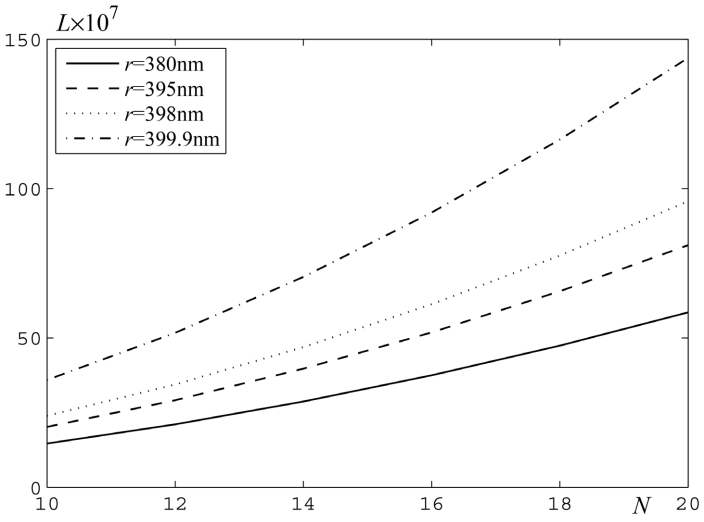

Figure 4. The self-inductance L at the values of r approaching to a.

5.2. Calculation of the Energy of Circular Solenoid

The numerical data presented in this Subsection are related to study of dependence of the energy flow produced by circular toroidal solenoid. The sketch of problem geometry is shown in Figure 5. The solenoid parameters are the following: the radius of torus is equal to 0.1 m, the inner radius of torus is equal to 0.10 m, $N = 10$, the value of current I in the solenoid coils are fixed as well, but it can be chosen also as the optimization parameter; the rest of geometrical and physical parameters are changing to define the optimal values of the radiated energy. The calculations are carried out in the vicinity of 6 GHz frequency. In the spherical coordinates, the element of volume is $\mathrm{d}V = r^2 \sin\theta \mathrm{d}r\mathrm{d}\theta\mathrm{d}\varphi$. The integration in Formula (20) is carried out numerically.

In Figure 6 and Figure 7, the values of E_θ and E_r components are shown at the distance 1 m from the torus center for the frequencies 6 GHz, 7 GHz, and 8 GHz. One can see that the amplitudes change considerably for the examined frequencies. It is turned out that the amplitude of E_θ increases when f grows, this increasing is reached about two times for the maximal amplitude. And for the E_r component it is vice versa: the amplitude decreases when f grows, and the rate of decreasing is more than ten times.

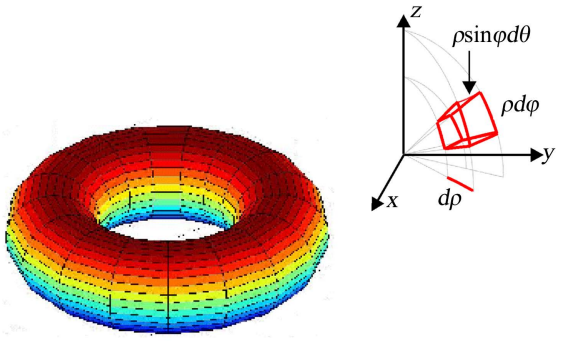

Figure 5. The geometry for calculating the energy value.

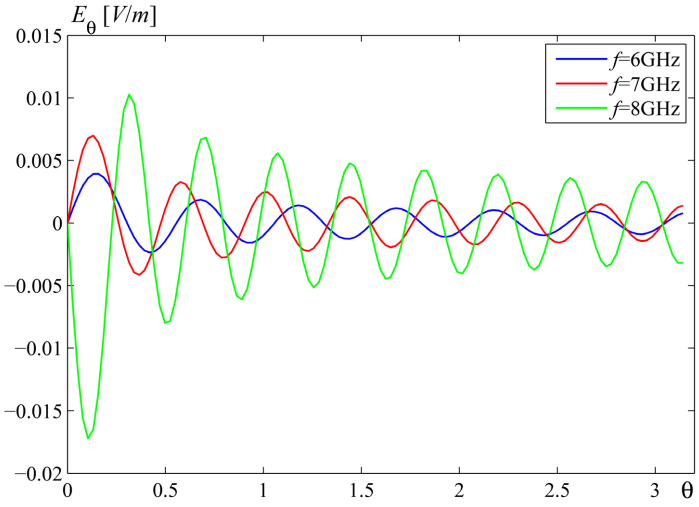

Figure 6. The component E_θ for the different frequencies f.

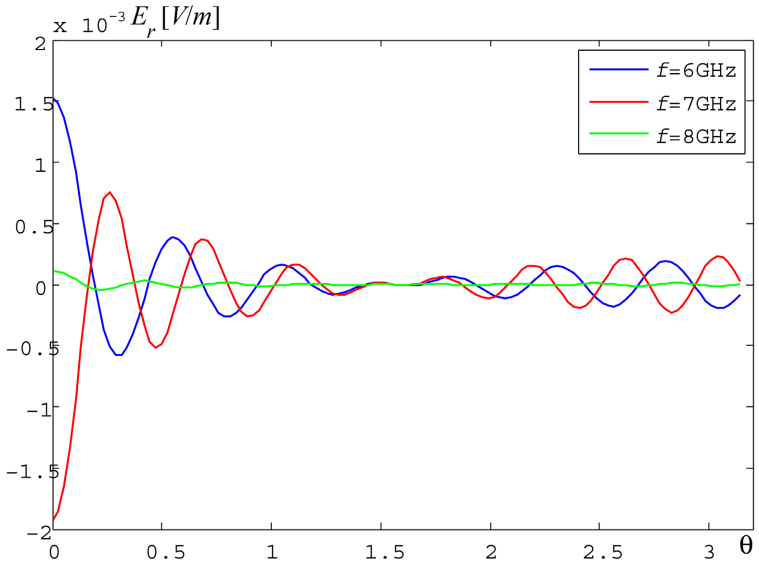

Figure 7. The component E_r for the different frequencies f.

In **Figure 8** and **Figure 9**, the typical amplitudes of the E_θ and E_r components are shown as function of r and θ arguments; the units of components is [V/m]. The values of coordinate r are changed from 0.5 m up to 5.0 m. The characteristic property of the E_θ is that the its value changes not considerably in sense of dependence on the r and θ coordinates and this change has periodical nature along the distance r; the dependence on θ is lower and it diminishes if r grows.

The property of the E_r component depends on the value of radius r in a great extent. So the maximal value of amplitude does not exceed 3×10^{-5} starting form $r = 4.5$ m. The characteristic property of the E_r component is concentration of radiation in the central direction $\theta = 0$. This means that the respective component of the pattern of radiation is narrow.

The peculiarity of energy distribution is studied at the different geometrical parameters of solenoid parameters. The domain V, in which the energy W_e is calculated, is defined as $V = \{0 \le \theta \le \pi/2, 0.5 \le r \le 5.0\}$ (r is measured in m). The dependence of the energy W_e (in Joule) on the frequency f at the different numbers N of coils in solenoid is shown in **Figure 10**. The property of W_e at such set of initial parameters is that the energy grows if the number N increases; simultaneously, it grows at the increasing of f. The results demonstrate the resonant character of W_e at the certain values of f. For example, the value of W_e tends to zero at $f = 5.95$ GHz, and the maximum is attained at the frequency $f = 7.93$ GHz. This allows us to determine the optimal values of the solenoid parameters providing the better performances from the energy efficiency point of view. The similar characteristics are got at the study dependence of W_e on the diameter d of torus (**Figure 11**). The energy W_e diminishes when diameter d grows. The above is explained by the physical nature of solenoid as the source of electromagnetic radiation: the energy is distributed in the larger volume, therefore this cannot concentrate the same portion of radiation in the same fixed volume.

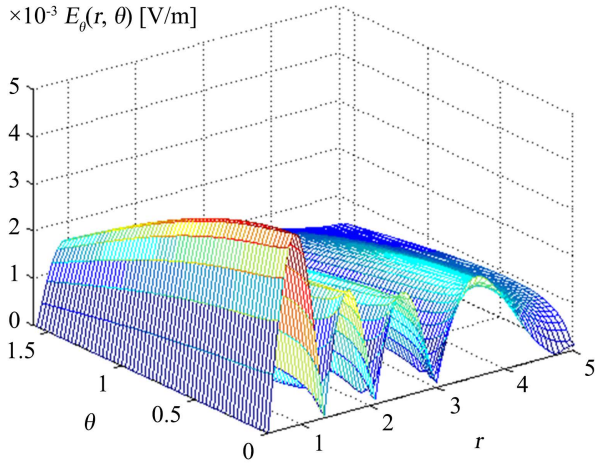

Figure 8. The component $E_\theta(r,\varphi)$ versus raduis r and angle θ.

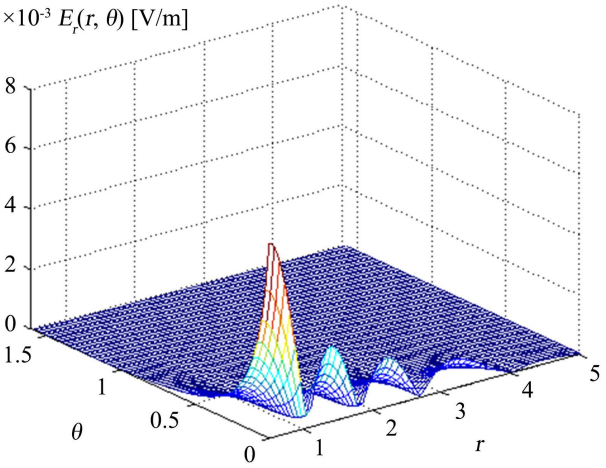

Figure 9. The component $E_r(r,\varphi)$ versus raduis r and angle θ.

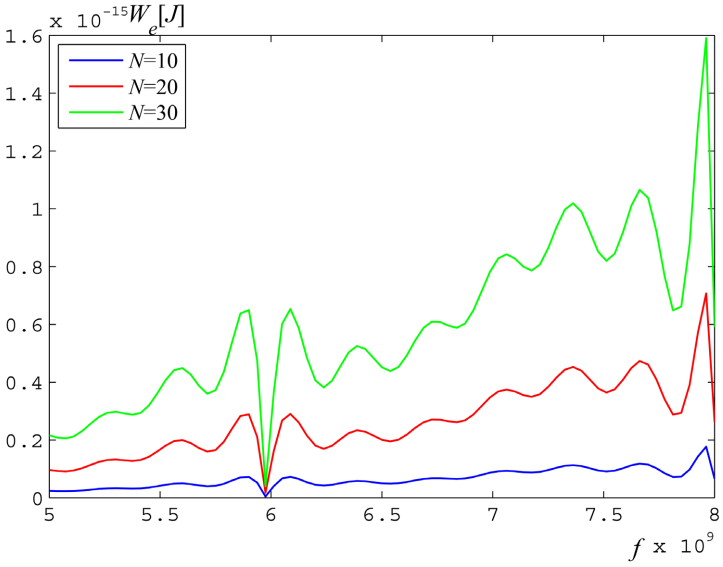

Figure 10. The energy W_e versus the frequency f at the different N.

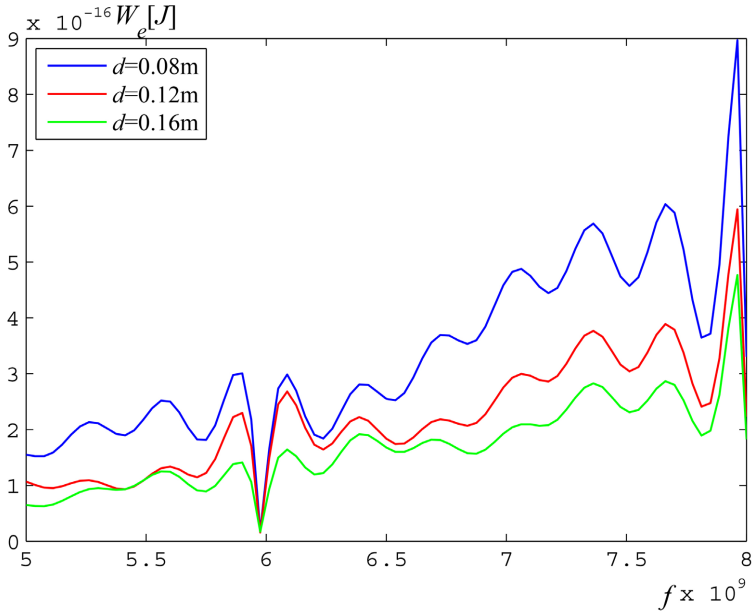

Figure 11. The energy W_e versus the frequency f at the different d.

The obtained results open a perspective to determination of the forces arisen at the functioning the micro devices supplemented by solenoids. It seems that the analytical determination of forces is not easy, but the numerical calculation using the Formulas (27) and (28) is attractive.

6. Conclusion

The modeling results related to study the electrical properties of the solenoids used for MEMS applications are presented in the paper. The investigation of the self-inductance of the rectangular microsolenoid demonstrates that there are the relations between the geometrical data of solenoid that provide the increase the self-inductance more that 30 times. The numerical data related to the calculation of the energy of the circular solenoid demonstrated the possibility to easy its calculation having the values of EM field components. The results can be extended on the case of the electrodynamical fields that foresees the supplementing Formula (20) by the usual additional term. The obtained results are suitable for modeling the run devices of MEMS, providing its necessary performances. The perspective of approach is ability to extend it on the calculation of the force characteristics of the motion parts of MEMS and to evaluate their reliability behaviors.

Conflicts of Interest

The authors declare no conflicts of interest regarding the publication of this paper.

References

[1] Verspecht, J., Horn, J., Betts, L., Gunyan, D., Pollard, R., Gillease, C. and Root, D.E.

(2009) Extension of X-Parameters to Include Long-Term Dynamic Memory Effects. 2009 *IEEE MTT-S International Microwave Symposium Digest*, Boston, 7-12 June 2009, 741-744. https://doi.org/10.1109/MWSYM.2009.5165803

[2] Senturia, S.D. (2001) Microsystem Design. Springer, New York. https://doi.org/10.1007/b117574

[3] Rebeiz, G.M. (2003) RF MEMS, Theory, Design and Technology. Wiley, Hoboken. https://doi.org/10.1002/0471225282

[4] Ventra, M.D., Pershin, Y.V. and Chua L.O. (2009) Circuit Elements with Memory: Memristors, Memcapacitors, and Meminductors. *Proceedings of the IEEE*, **97**, 1717-1724. https://doi.org/10.1109/JPROC.2009.2021077

[5] Mestrom, R.M.C., Fey, R.H.B. and Nijmeijer, H. (2009) Phase Feedback for Nonlinear MEM Resonators in Oscillator Circuits. *IEEE/ASME Transactions on Mechatronics*, **14**, 423-433. https://doi.org/10.1109/TMECH.2009.2023447

[6] Kaajakari, V., Mattila, T., Lipsanen, A. and Oja, A. (2004) Nonlinear Mechanical effects in Silicon Longitudinal Mode Beam Resonators. *Sensors and Actuators A*: *Physical*, **120**, 64-70. https://doi.org/10.1016/j.sna.2004.11.010

[7] Kaajakari, V., Mattila, T., Oja, A., Kiihamäki, J. and Seppä, H. (2004) Square-Extensional Mode Single-Crystal Silicon Micromechanical Resonator for Low-Phase-Noise Oscillator Applications. *IEEE Electron Device Letters*, **25**, 173-175. https://doi.org/10.1109/LED.2004.824840

[8] Kaajakari, V., Koskinen, J.K. and Mattila, T. (2005) Phase Noise in Capacitively Coupled Micromechanical Oscillators. *IEEE Transactions on Ultrasonics, Ferroelectrics, and Frequency Control*, **52**, 2322-2331. https://doi.org/10.1109/TUFFC.2005.1563277

[9] Holmgren, O., Kokkonen, K., Veijola, T., Mattila, T., Kaajakari, V., Oja, A., Knuuttila, J.V. and Kaivola, M. (2009) Analysis of Vibration Modes in a Micromechanical Square-Plate Resonator. *Journal of Micromechanics and Microengineering*, **19**, Article ID: 015028. https://doi.org/10.1088/0960-1317/19/1/015028

[10] DeMartini, B.E., Butterfield, H.E., Moehlis, J. and Turner, K.L. (2007) Chaos for a Microelectromechanical Oscillator Governed by the Nonlinear Mathieu Equation. *Journal of Microelectromechanical Systems*, **16**, 1314-1323. https://doi.org/10.1109/JMEMS.2007.906757

[11] Mestrom, R.M.C., Fey, R.H.B. and Nijmeijer, H. (2007) On Phase Feedback for Nonlinear MEMS Resonators. *IEEE International Frequency Control Symposium Joint with the* 21*st European Frequency and Time Forum*, Geneva, 29 May-1 June 2007, 765-770. https://doi.org/10.1109/FREQ.2007.4319179

[12] Lyshevski, S.E. (2000) Nano- and Micro-Electromechanical Systems: Fundamentals of Nano- and Microengineering. 2nd Edition, CRS Press, Boca Raton, London, New York, Washington.

[13] Afanasiev, O.N. and Dubovik, V.M. (1992) Electromagnetic Properties of Toroidal Solenoid. *Journal of Physics A*: *Mathematical and General*, **25**, 4869-4886. https://doi.org/10.1088/0305-4470/25/18/020